AFRL-RH-WP-TR-2021-0045

Development of a Radon Background Subtraction Algorithm for the Electronic Personal Dosimeter

Alexander Brandl

Colorado State University

AUGUST 2021
Final Report

AIR FORCE RESEARCH LABORATORY
711TH HUMAN PERFORMANCE WING,
AIRMAN SYSTEMS DIRECTORATE,
WRIGHT-PATTERSON AIR FORCE BASE, OH 45433
AIR FORCE MATERIEL COMMAND
UNITED STATES AIR FORCE

NOTICE AND SIGNATURE PAGE

Using Government drawings, specifications, or other data included in this document for any purpose other than Government procurement does not in any way obligate the U.S. Government. The fact that the Government formulated or supplied the drawings, specifications, or other data does not license the holder or any other person or corporation; or convey any rights or permission to manufacture, use, or sell any patented invention that may relate to them.

This report was cleared for public release by the Air Force Research Laboratory Public Affairs Office and is available to the general public, including foreign nationals. Copies may be obtained from the Defense Technical Information Center (DTIC) (http://www.dtic.mil).

AFRL-RH-WP-TR-2021-0045 HAS BEEN REVIEWED AND IS APPROVED FOR PUBLICATION IN ACCORDANCE WITH ASSIGNED DISTRIBUTION STATEMENT

HORENZIAK.MICHAEL.W.1256763911 Digitally signed by HORENZIAK.MICHAEL.W.1256763911 Date: 2021.09.29 11:20:48 -04'00'

MICHAEL W. HORENZIAK, Maj, USAF
Force Health Protection Section
Airman Biosciences Division
Airman Systems Directorate

YAMAMOTO.DIRK.P.1138663511 Digitally signed by YAMAMOTO.DIRK.P.1138663511 Date: 2021.09.29 12:18:47 -04'00'

DIRK P. YAMAMOTO, DR-III, PhD
Chief, Force Health Protection Section
Product Development Branch
Airman Biosciences Division

This report is published in the interest of scientific and technical information exchange, and its publication does not constitute the Government's approval or disapproval of its ideas or findings.

REPORT DOCUMENTATION PAGE

Form Approved
OMB No. 0704-0188

1. REPORT DATE *(DD-MM-YYYY)*	2. REPORT TYPE	3. DATES COVERED *(From – To)*
24-08-2021	Final Report	Janurary - June 2020

4. TITLE AND SUBTITLE
Development of a Radon Background Subtraction Algorithm for the Electronic Personal Dosimeter

5a. CONTRACT NUMBER
S-145-305-001

5b. GRANT NUMBER

5c. PROGRAM ELEMENT NUMBER

6. AUTHOR(S)
[1] Alexander Brandl, PhD, CHP

5d. PROJECT NUMBER

5e. TASK NUMBER

5f. WORK UNIT NUMBER
Legacy RHM

7. PERFORMING ORGANIZATION NAME(S) AND ADDRESS(ES)
[1] Colorado State University, Department of Environmental & Radiological Health Sciences, 1601 Campus Delivery, Fort Collins CO, 80523-1601

8. PERFORMING ORGANIZATION REPORT NUMBER

9. SPONSORING / MONITORING AGENCY NAME(S) AND ADDRESS(ES)
Air Force Materiel Command
Air Force Research Laboratory
711th Human Performance Wing
Airman Systems Directorate
Airman Biosciences Division
Product Development Branch
Wright-Patterson AFB, OH 45433

10. SPONSORING/MONITOR'S ACRONYM(S)
711 HPW/RHBAF

11. SPONSOR/MONITOR'S REPORT NUMBER(S)
AFRL-RH-WP-TR-2021-0045

12. DISTRIBUTION / AVAILABILITY STATEMENT
DISTRIBUTION STATEMENT A. Approved for public release.

13. SUPPLEMENTARY NOTES
AFRL-2021-2870, cleared 26 Augsut 2021

14. ABSTRACT

The work provided by Colorado State University (CSU) under subcontract encompasses the development of an algorithm to subtract radon (Rn) background from the reading provided by electronic personal dosimeters (EPDs). This allows users / operators to distinguish ubiquitous natural radiation signals from man-made sources of ionizing radiation potentially of concern.

A generic mathematical / statistical formalism for the algorithm was derived by consideration of the raw data / signals expected from any two-channel EPD. While this algorithm is generic in nature and specific to the set of detector geometry assumptions detailed below, it is also universal. It is applicable to any detection system utilizing at least two independent measurements of ionizing radiation in the immediate environment of the user / operator conducted with different β/γ-attenuators. For an effective and accurate algorithm, the detector and attenuator specifications need to be known for the computation of the requisite algorithm input parameters. CSU has not been privy to such manufacturer specifications during the course of this project, so the algorithm was developed using the physical basis for detector response and was benchmarked for different sets of assumptions pertaining to the design of electronic personal dosimeters with two silicon detectors and attenuators commonly used in the industry.

Earlier generic assumptions were expanded to also include other design options, which allows the sponsor to gain an understanding of the influence factors pertaining to their specific make and model of EPD. If detector and attenuator information for a specific EPD can be shared with CSU, they will provide a tailored algorithm for the instrument at hand.

15. SUBJECT TERMS
Algorithm, background radon, electronic personal dosimeter

16. SECURITY CLASSIFICATION OF:			17. LIMITATION OF ABSTRACT	18. NUMBER OF PAGES	19a. NAME OF RESPONSIBLE PERSON
a. REPORT	b. ABSTRACT	c. THIS PAGE			Major Michael Horenziak
U	U	U	SAR	16	19b. TELEPHONE NUMBER *(include area code)* N/A

Standard Form 298 (Rev. 8-98)
Prescribed by ANSI Std. Z39.18

TABLE OF CONTENTS

LIST OF FIGURES

Page

LIST OF TABLES

Page

1.0 SUMMARY/ABSTRACT

Colorado State University (CSU) is submitting the final report for Subcontract S-145-305-001 with a reporting period of 01JAN20 to 30JUN20. The project was completed by the end of the reporting period. This final report contains the results of the final data analysis and compilation of those data for the sponsor's perusal.

The work provided by CSU under this subcontract encompasses the development of an algorithm to subtract radon (Rn) background from the reading provided by electronic personal dosimeters (EPD). This allows users / operators to distinguish ubiquitous natural radiation signals from man-made sources of ionizing radiation potentially of concern.

A generic mathematical / statistical formalism for the algorithm was derived by consideration of the raw data / signals expected from any two-channel EPD. While this algorithm is generic in nature and specific to the set of detector geometry assumptions detailed below, it is also universal. It is applicable to any detection system utilizing at least two independent measurements of ionizing radiation in the immediate environment of the user / operator conducted with different β/γ-attenuators. For an effective and accurate algorithm, the detector and attenuator specifications need to be known for the computation of the requisite algorithm input parameters. CSU has not been privy to such manufacturer specifications during the course of this project, so the algorithm was developed using the physical basis for detector response, and was benchmarked for different sets of assumptions pertaining to the design of electronic personal dosimeters with two silicon detectors and attenuators commonly used in the industry.

Earlier generic assumptions were expanded to also include other design options, which allows the sponsor to gain an understanding of the influence factors pertaining to their specific make and model of EPD. If detector and attenuator information for a specific EPD can be shared with CSU, they will provide a tailored algorithm for the instrument at hand.

2.0 INTRODUCTION/BACKGROUND

Many first responders have been outfitted with electronic personal dosimeters (EPD) to respond to a variety of accident and incident scenarios, and threats to public safety, some of which may include radiological or nuclear hazards. EPDs allow them to recognize and identify a radiological hazard during their response operations (e.g., orphan radiological source, radiological dispersal device, improvised nuclear device).

General "force protection" is accomplished by EPDs reading in the quantities dose rate or cumulative dose [2, 5] and alerting the first responder to the exceedance of pre-set alarm levels. The first responder thus carries the technical capabilities to assess the radiological situation and take the appropriate protective measures for themselves and other individuals in the immediate proximity. At the same time, however, EPDs do not provide information about the nature of the radiological source and do not distinguish between various contributions to the instrument reading. In certain situations, such as upon entering a building, basement, tunnel, or area where a background reading was established from an outside environment, additional information would be necessary for a more informed interpretation of an EPD reading. Increased instrument readings could indicate the presence of an anthropogenic radiological source, or could be misinterpreted as a change in natural background in the presence of a radiological source such as a well shielded Radiological Disposal Device (RDD) or Improvised Nuclear Device (IND). In either case the user / operator might miss critical information for prudent execution of their mission. The identification and subtraction of Rn background provides greater confidence to the first responder.

The general approach to radon background subtraction developed in this study is applicable to any radon isotope and their progeny, or mixtures thereof. Due to the relative radiological half-lives of the various radon isotopes in the natural environment, current algorithm development has neglected airborne concentrations of ^{220}Rn and ^{219}Rn and their progeny compared to the concentration of ^{222}Rn and progeny. The algorithm / model readily can be amended to accommodate the other isotopes of radon if they were suspected to be present in non-negligible concentrations.

Commercially available detection systems for radon and progeny employ passive as well as active methods [11], which either require sample analysis in a laboratory, or are cumbersome to use and not suitable for deployment under field conditions. In either case, they do not provide real-time actionable information to the user / operator. Background measurements obtained by an EPD prior to accessing a building may not be valid inside, or if not measured concurrently may not reflect the accurate and local radon levels in the first responder's immediate proximity [13]. Real-time analysis of the radon progeny contribution to the EPD reading will allow a more confident interpretation of the display values by the first responder.

The detection media in EPDs frequently are either Geiger-Mueller counters or solid state detectors (e.g., silicon) [1, 2, 5, 7]. Often, they contain more than one independent detector (channels) [5]. Multi-channel instruments with different filters for the various channels, at the level of simple signal recognition, provide additional information on the nature of the incident ionizing radiation which can be used to assess the signal contribution from radon progeny. Our generic algorithm was developed for a simple two-channel EPD. Algorithm component variables are shown in a schematic representation in Figure 1.

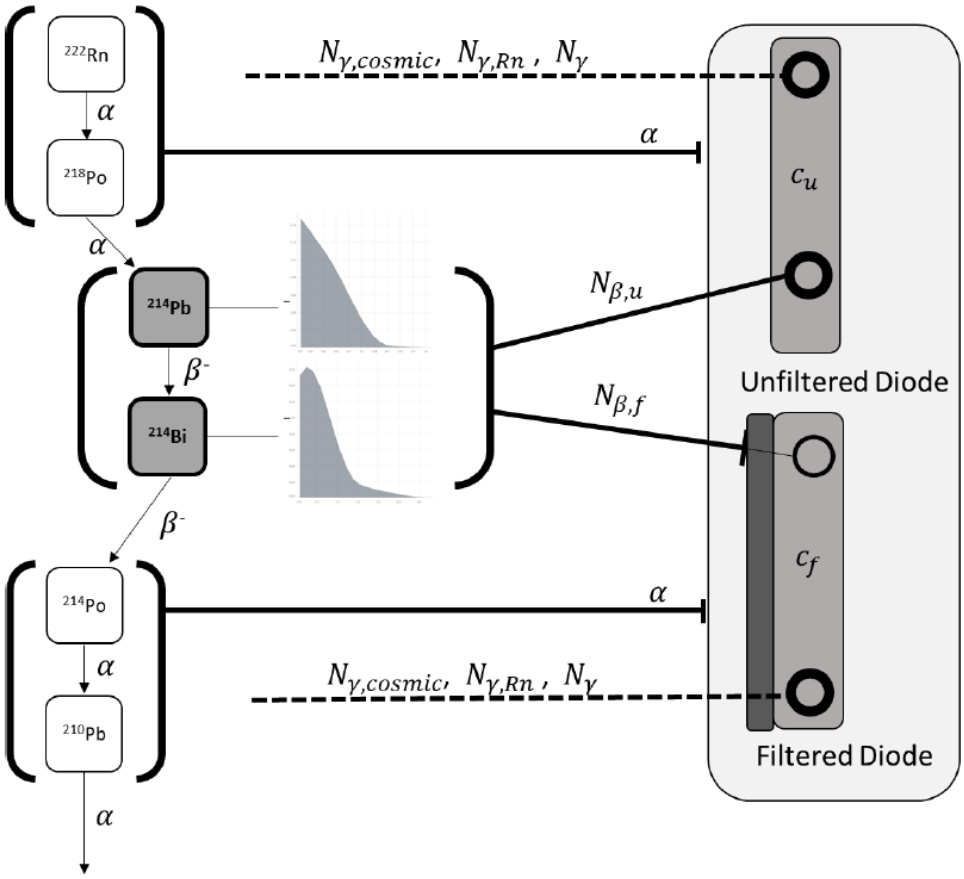

Figure 1: Radon and radon daughter contributions to the natural radiation environment

Our algorithm utilizes the correlation from beta and gamma contributions from radon progeny to the number of signal events ("counts") observed between the two channels; neither the actual ^{222}Rn concentration nor the equilibrium factor [4] need to be known. To model the detector response, the CSU team utilized the Monte Carlo N-Particle (MCNP) Transport code [9], but any suitable radiation transport code could serve for this purpose. While the algorithm developed is universal in nature, the detector response model is specific to the instrument geometry, detectors employed, and filters, and will need to be re-evaluated for different EPD makes and models. In our generic model, ^{222}Rn progeny are in secular equilibrium to ^{210} Lead (Pb). No other airborne beta emitters in proximity of the EPD are included. Should additional information be available on processes which would alter the radon progeny equilibrium and / or airborne beta concentrations, the algorithm can be adapted correspondingly.

CSU has not been privy to manufacturer specifications for the detectors and filters. For the generic algorithm, however, the CSU team modeled a typical EPD geometry with two silicon diode detectors, each covered by a thin Mylar® window. The unfiltered diode for beta detection does not include any additional filter material. The filtered diode is covered by three layers of filter material to flatten the energy response to incident gamma radiation [6, 12]. The filter design follows reports in the literature [8], and consists of 0.08 millimeter (mm) of Tantalum (Ta), 0.2 mm of Tin (Sn), 0.5 mm of copper (Cu), and 0.5 micrometer (μm) of Al (metallization layer).

The preliminary model described above subsequently was updated and expanded to represent a more sophisticated geometry for the filtered and unfiltered silicon diodes. While the previous models of the unfiltered diode contained a silicon active volume protected by a Mylar® filter only, the refined geometry is expected to be a closer representation of a modern EPD in both size and material composition. A depiction of the updated unfiltered diode is shown in Fig. 2, and reflects the optimal composition of silicon pin diodes for detecting photons [8]. Additional layers of Cu, Sn, and Ta were used to create the filtered diodes for this geometry. A Silicon Dioxide (SiO_2) layer was added to both the unfiltered and filtered diodes.

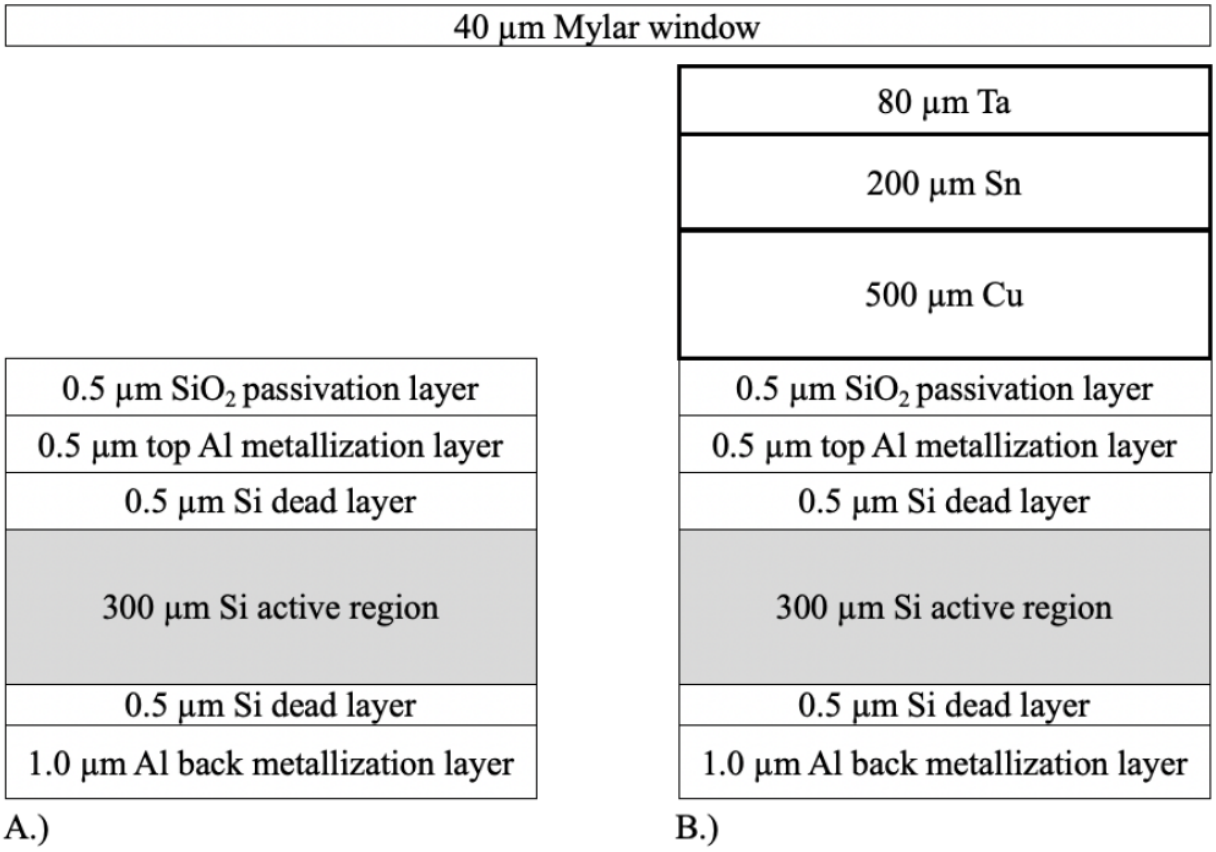

Figure 2: Schematic and material composition of A) the unfiltered and B) the filtered silicon diodes modeled in MCNP (drawing not to scale)

3.0 METHODS

The preliminary model was evaluated using Monte Carlo N-Particle eXtended (MCNPX) in the MCNP suite of computer codes. The most recent simulations were performed with an updated version of MCNP, MCNP6, for the radiation transport simulation. MCNP6 builds upon the previous versions of MCNP and includes the most up-to-date scientific data to compute radiation transport and interactions.

The sampling volume for ^{222}Rn and progeny surrounding the detector is 1 cubic meter (m^3). The face of each diode measured 10 mm × 10 mm; the thickness of the detector and protective or shielding layers in the most recent simulations was 0.3 mm for the unfiltered and 1.1 mm for the filtered diodes. The active volume of the detectors could be considered rather small but is representative of a physical EPD. A Mylar® window was placed at the same distance between the radiation source and the silicon diodes for both the unfiltered and the filtered detectors.

^{222}Rn and progeny emit alpha and beta particles as well as gamma radiation. For alpha, emission, only 7.69 Mega Electron-Volts (MeV) monoenergetic alphas were simulated with MCNP, as they represent the highest energy alphas associated with ^{222}Rn progeny decay. The beta energy spectra associated with the decay of ^{214} Bismuth (Bi) and ^{214}Pb, detailed in International Commission on Radiological Protection (ICRP) 107 [3], were used for the two separate MCNP beta runs. A correction factor of 0.6704 was introduced for the ^{214}Bi results to account for its reduced beta yield. The gamma energy spectrum and associated emission probabilities for the progeny of ^{222}Rn were extracted from the literature[10]. The MCNP tallies were defined within the active region of the filtered and unfiltered silicon diodes. The output sum of the results from the ^{214}Bi and ^{214}Pb beta simulations, and the results for the gamma simulations were determined for the unfiltered and filtered diodes.

The generic EPD for modeling and benchmarking utilizes a configuration of two silicon diodes covered by different filters. Photon contributions from the ^{222}Rn progeny are discriminated by comparison of the signals obtained in the two channels. The more heavily filtered silicon diode is used to model the detector response to gamma radiation, and the "unfiltered" silicon diode is used to model the detector response to airborne beta particles and low-energy gammas.

The data analysis for radon background subtraction has to occur at the level of the primary detector response ("counts"), i.e., prior to the electronic display of the dose rate or dose in the instrument, and prior to other manufacturer-supplied convolution or calibration algorithms. The algorithm does not consider beta interactions in the detector other than those from ^{222}Rn progeny.

The Monte Carlo model of the detector response directly provides the expected ratio of ^{222}Rn progeny gamma interactions versus the ^{222}Rn progeny beta interactions on the unfiltered diode ($k_{\gamma\beta,exp}$), and the expected ratio of beta interactions on the unfiltered diode versus beta interactions on the filtered diode ($k_{\beta,exp}$) for the ^{222}Rn progeny. These computed ratios are sufficient to derive an algorithmic process to subtract the gamma ray contributions from ^{222}Rn and its progeny.

CSU has not been privy to manufacturer specifications for the detectors and filters. For the generic algorithm, however, the CSU team modeled typical EPD geometries with two silicon diode detectors, each covered by a thin Mylar® window.

4.0 RESULTS AND DISCUSSION

Using the number of interactions modeled for each silicon diode, the expected total number of interactions per ^{222}Rn progeny decay is obtained for each diode. Simulated 7.69 MeV monoenergetic alpha particles did not reach and interact in the active volumes of the unfiltered or filtered diodes. Further consideration was only given to beta particles and gammas associated with ^{222}Rn progeny decay.

The expected total number of interactions in the filtered silicon diode per ^{222}Rn progeny decay is calculated by adding the expected number of interactions obtained in the filtered diode from the different γ- and β- emitting progeny, and is denoted $c_{f,\mathrm{exp}}$. Similarly, the expected total number of interactions on the unfiltered silicon diode per ^{222}Rn progeny decay, $c_{u,\mathrm{exp}}$, is obtained as the sum of all simulated interactions in the unfiltered diode. The number of gamma interactions on both silicon diodes is expected to vary slightly due to the additional shielding on the filtered diode, giving rise to the gamma ray correction factor, ε_{exp}, which is computed by the ratio of the expected number of gamma interaction in the filtered and in the unfiltered silicon diodes. The quantities c_f, c_u, and ε are related by the following expressions for any measurement utilizing an EPD with two channels:

$$c_u = N_{\beta,u} + N_\gamma, \text{ and} \tag{1}$$

$$c_f = N_{\beta,f} + \varepsilon N_\gamma, \tag{2}$$

where N_β and N_γ are the number of interactions from betas and gammas in the detectors, respectively. The subscript exp denotes an "expected" quantity, the numerical value of which is obtained from the geometry and model-specific MCNP simulation, not by a physical measurement.

If all beta interactions in the detectors result from ^{222}Rn progeny decay in the ambient air surrounding the EPD, the measured number of beta interactions on the two silicon diodes will equal the expected number of beta interactions on them, or $k_\beta = k_{\beta,exp}$ such that

$$k_\beta = \frac{N_{\beta,u,exp}}{N_{\beta,f,exp}} = \frac{N_{\beta,u}}{N_{\beta,f}} = \frac{c_u - N_\gamma}{c_f - \varepsilon N_\gamma}, \text{ or} \tag{3}$$

$$N_\gamma = \frac{c_u - k_\beta c_f}{1 - k_\beta \varepsilon}, \tag{4}$$

where N_γ is defined as before, and k_β and ε result from the Monte Carlo simulation of the EPD geometry. However, N_γ now is independent of the origin of the gamma emission, thus not necessarily associated only with the decays from ^{222}Rn progeny, and can account for other sources for gamma signals in the EPD if c_u and c_f are the measured number of interactions on the unfiltered and filtered silicon diodes, respectively, during instrument deployment.

Since N_γ has been determined, , can be obtained by inversion of Eqn. 1 for any EPD measurement, provided the total number of interactions on the unfiltered silicon diode is known. The ratio of the expected number of ^{222}Rn progeny gamma interactions, $N_{\gamma,}$, and $N_{\beta,u}$ is fixed at $k_{\gamma\beta,exp}$, such that

$$N_{\gamma,Rn} = k_{\gamma\beta,exp} N_{\beta,u} \tag{5}$$

The result in Eqn. 5 provides a basis for distinguishing between signal contributions from

gammas originating from ^{222}Rn progeny decay and from other gamma sources, i.e., from cosmic ray background:

$$N_{\gamma,cosmic} = N_{\gamma} - N_{\gamma,Rn} \tag{6}$$

Local movement by a first responder, e.g., from a location outside a building to the inside, or between rooms within a building, will likely not alter the cosmic ray gamma signal significantly. An excess of gamma signal in the EPD, $N_{\gamma,}$ such that

$$N_{\gamma,EPD} > N_{\gamma,Rn} + N_{\gamma,cosmic} \tag{7}$$

indicates an unidentified gamma source in the proximity of the first responder. Fig. 3 visualizes the functional components of the algorithm in a block diagram.

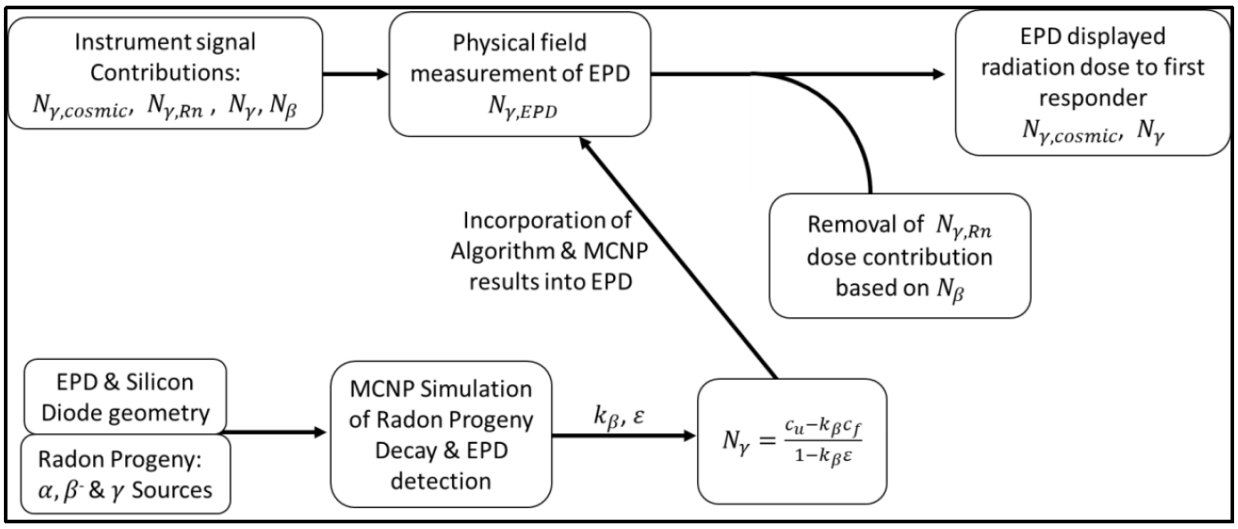

Figure 3: Block diagram for the radon background subtraction algorithm

Modeling results for k_{β}, $k_{\gamma\beta,}$, and ε for the preliminary generic EPD geometry utilizing two silicon diodes and for he expanded EPD geometry are provided in Tables 1 and 2, respectively.

Table 1: Model results for the main parameters for radon background subtraction in the preliminary generic EPD geometry

Model EPD	
k_{β}	9.448
$k_{\gamma\beta,exp}$	0.985
ε	0.954

Table 2: Model results for the main parameters for radon background subtraction in the expanded generic EPD geometry

Model EPD	
k_β	6.81
$k_{\gamma\beta,exp}$	1.05
ε	0.982

The results in Table 2 as compared to those in Table 1 provide evidence that both the size and the composition of the silicon diodes utilized by the EPD impact the values of k_β, $k_{\gamma\beta,exp}$, and ε. This, however, is to be expected. As two major geometrical parameters were changed, the size of both the filtered and unfiltered diodes and the composition, thicknesses, and layers of the shielding materials, the results varied significantly.

The previously unfiltered diode consisted of only the silicon active volume. The incorporation of the additional layers, as shown in Fig. 1, increases the attenuation of beta particles, thus reducing the amount of beta particle interactions within the active volume of the unfiltered diode. The filtered diode also added layers of filtration between the source of radiation and the active volume of the detector which similarly reduces the number of interactions due to beta particles from ^{222}Rn progeny decay. The reduced k_β value can be attributed to a decreased probability of beta interaction within the active volume of the unfiltered diode.

For the operational implementation of this algorithm, the most recent results confirm the algorithm's ability to distinguish signal contributions from gammas originating from ^{222}Rn progeny decay and from other gamma sources. At the same time, however, they also show the importance of proper modeling of the specific geometries of the chosen EPD. Variances between the composition and size of a two-channel silicon diode EPD impact the computed values for k_β, $k_{\gamma\beta,exp}$, and ε which are integral to distinguishing these two possible gamma signal contributions. Importantly, the expanded detector system was derived from studies with the objective to optimize the detection of photons. Accordingly, being that this algorithm relies on the detection of beta particles from ^{222}Rn progeny decay, further research should be focused towards optimizing the beta particle detection component as well.

Results were checked for internal consistency and validated by using MCNP-generated values for c_u and c_f, including an additional contribution from gammas with an energy of 662 Kiloelectron Volts (keV) to simulate an orphan ^{137}Cs source, and determining the level of requisite ^{222}Rn progeny background subtraction and excess gamma contribution.

All validation and benchmarking steps performed satisfactorily.

5.0 CONCLUSION

A radon background subtraction algorithm for EPDs, such as those frequently worn by various first responders, has been developed. Numerical values computed for the main parameters in the algorithm are specific to the EPD configuration. However, the approach is universally applicable, only requiring a computational radiation transport model of the actual EPD geometry. Active real-time radon background subtraction allows the first responder to maintain their focus on their operational necessities without undue distraction from readings of a changing radon background and the uncertain interpretation of the EPD display value.

Our radon background discrimination algorithm uses a limited set of assumptions. A necessity for employment of our algorithm is that the EPD contains at least two independent detectors with different filters. Our results emphasize the importance of a well-defined system geometry and composition. Numerical values utilized in our algorithm were generated from detector models designed only for the purpose of this study, and were subsequently implemented in radiation transport modeling; application of the algorithm to an EPD ready for deployment will require instrument-specific modeling of its geometry. Any beta particles detected by the EPD are assumed to be the result of the decay of radon progeny; no other airborne sources of beta emission are present in close proximity to the first responder. The short-lived radon progeny emitting betas and gammas are in secular equilibrium; however, the equilibrium factor between radon gas and suspended particulate radon progeny does not need to be known. For location-specific information which indicates that these assumptions need to be relaxed or modified, an updated model computation readily can account for such a change in circumstances. However, the real-time advantage of this radon background subtraction may be lost. Alternatively, manufacturers could develop menu options which would consider different operational scenarios, utilizing pre-computed algorithm input parameters.

Implementation of our radon background subtraction algorithm requires mathematical manipulation of the instrument raw data at the level of the number of interactions by ionizing radiation in the two detectors (“counts”). If the data have been energy compensated or manipulated in any other way, the results may not be accurate.

6.0 REFERENCES

[1] Adachi, N., Adamovitch, V., Adjovi, Y., Aida, K., H, A., S, A., . . . M, K. (2016). Measurement and comparison of individual external doses of high-school students living in Japan, France, Poland and Belarus – the "D-shuttle" project. *Journal of Radiological Protection, 36*(1), 49-66. doi:10.1088/0952-4746/36/1/49

[2] Barthe, J. (2001, September 24). Electronic dosimeters based on solid state detectors. *Nuclear Instruments and Methods in Physics Research B, 184*, 158-189. doi:https://doi.org/10.1016/S0168-583X(01)00711-X

[3] International Commission on Radiological Protection. (2008). Nuclear decay data for dosimetric calculations. *ICRP Publication 107, Annals of the ICRP, 38*(3). Retrieved from https://www.icrp.org/publication.asp?id=ICRP%20Publication%20107

[4] International Commission on Radiological Protection. (2010). Lung cancer risk from radon and progeny and statement on radon. *ICRP Publication 115, Annals of the ICRP, 40*(1). Retrieved from https://www.icrp.org/publication.asp?id=icrp%20publication%20115

[5] Krzanovic, N., Zivanovic, M., Ciraj-Bjelac, O., Lazarevic, D., Ceklic, S., & Stankovic, S. (2017, October). Performance testing of selected types of electronic personal dosimeters in x- and gamma radiation fields. *Health Physics, 113*(4), 252-261. doi:10.1097/HP.0000000000000704

[6] Lee, B. J., Lee, W., Cho, G., Chang, S. Y., & Rho, S. R. (2003). Solid-state personal dosimeter using dose conversion algorithm. *Nuclear Instruments and Methods in Physics Research A, 505*(1-2), 403-406.

[7] Meier, J., & Cheenu Kappadath, S. (2015, November). Characterization of the energy response and backscatter contribution for two electronic personal dosimeter models. *Journal of Applied Clinical Medical Physics, 16*(6), 423-434. doi:10.1120/jacmp.v16i6.5549

[8] Mitra, P., Srivastava, S., Singh, K. S., Akar, K. D., Patni, K. H., Topkar, A., & Kumar, V. A. (2016, December). Optimum energy compensation for current mode application of silicon PIN diode in gamma radiation detection. *IEEE Transactions on Nuclear Science, 63*(6), 2777-2781. Retrieved from https://www.researchgate.net/publication/309541268_Optimum_Energy_Compensation_for_Current_Mode_Application_of_Silicon_PIN_Diode_in_Gamma_Radiation_Detection

[9] Monte Carlo N-Particle eXtended Team. (2008). Monte Carlo n-particle extended. Los Alamos: Los Alamos National Laboratory.

[10] Morel, J., Etcheverry, M., & Picolo, J. L. (1998, September). Main gamma-rays emission probabilities of radon-222 daughters. *Bulletin du Bureau National de Metrologie, 114*, 15-20.

[11] Nastro, V., Carni, D., Vitale, A., Lamonaca, F., & Vasile, M. (2018). Passive and active methods for radon pollution measurements in historical heritage buildings. *Measurement, 114*, 526-533.

[12] Sinclair, F., Clapp, A., & Entine, G. (1988, February). Energy compensated solid state gamma dosimeter. *IEEE Transactions on Nuclear Science, 35*(1), 562-566. doi:10.1109/23.12786

[13] Tommasone Pascale, F., De Francesco, S., Carbone, P., Cuoco, E., & Tedesco, D. (2014, July). Dry soil diurnal quasi-periodic oscillations in soil 222Rn concentrations. *Radiation Measurements, 66*, 31-41. doi:https://doi.org/10.1016/j.radmeas.2014.02.022

7.0 LIST OF SYMBOLS, ABBREVIATIONS AND ACRONYMS

Al	Aluminium
β	Beta
Bi	Bismuth
CSU	Colorado State University
Cu	Copper
EPD	Eletronic Personal Dosimeter
exp	Expected
γ	Gamma
ICRP	International Commission on Radiological Protection
keV	Kiloelectron Volts
m^3	Meters Cubed
μm	micrometre
MCNP	Monte Carlo N-Particle
MCNPX	Monte Carlo N-Particle eXtended
MeV	Mega Electron-Volts
mm	Millimeter
Pb	Lead
Rn	Radon
SiO_2	Silicon Dioxide
Sn	Tin
Ta	Tantalum